Effect of Formation Temperature and Roughness on Surface Potential of Octadecyltrichlorosilane Self-Assembled Monolayer on Silicon Surfaces†

Brian G. Bush, Frank W. DelRio, Justin Opatkiewicz, Roya Maboudian,* and Carlo Carraro

Department of Chemical Engineering, University of California, Berkeley, California 94720

Received: July 10, 2007; In Final Form: October 16, 2007

Kelvin probe force microscopy (KPFM) and atomic force microscopy (AFM) are employed to probe the surface potential and topography of octadecyltrichlorosilane [OTS, $CH_3(CH_2)_{17}SiCl_3$] self-assembled monolayers (SAMs) on oxidized Si(100) and polycrystalline silicon surfaces as a function of deposition temperature and substrate roughness with particular attention paid to the monitoring of SAM adsorption on highly rough surfaces. In these studies, it is found that the surface potential magnitude of the adsorbed layer is larger for monolayers formed in the liquid-condensed (LC) phase than for those formed in the liquid-expanded (LE) phase. Experiments on individual islands in the LC phase show that surface potential and monolayer thickness increase with increasing island size; islands larger than about 1.5 μm reach maximum potential and height values of 48 ± 4 mV and 2.7 ± 0.1 nm, with respect to the underlying oxidized surface. It is also shown that KPFM is suitable for the study of monolayer adsorption on polycrystalline surfaces, for which preexisting surface texture makes the use of traditional scanning probe techniques for molecular recognition difficult. In these scenarios it is shown that OTS growth occurs preferentially along grain boundaries in fingerlike patterns having a molecular arrangement comparable to that of LC phase islands on atomically smooth silicon. These findings indicate that surface potential measurements provide a highly accurate, local means of probing monolayer morphology on rough surfaces encountered in many applications.

Introduction

Self-assembly has long been exploited to produce monolayer films on solid surfaces in order to control the physical and chemical properties of the substrate.[1,2] Self-assembled monolayers (SAMs) prepared from alkylsiloxane molecules have shown promise for use as resist layers in various lithographic techniques,[3] as passivation layers for area selective atomic layer deposition,[4,5] as novel gate insulators in organic thin-film transistors,[6] and as molecular boundary lubricants in micromechanical devices.[7,8] To date, the growth kinetics of monolayer films, such as those prepared from octadecyltrichlorosilane [OTS, $CH_3(CH_2)_{17}SiCl_3$], have been studied extensively on atomically smooth silicon surfaces.[9−12] However, SAMs are frequently employed on surfaces that are rough, such as polycrystalline silicon[7] (polysilicon), and it remains unclear how alkylsiloxane films form on surfaces in which the roughness is on the order of, or higher than, the monolayer chain length. In these scenarios, topography-based scanning probe techniques are of little use as it becomes impossible to discern SAMs from preexisting surface texture.

In the past decade, a novel scanning probe technique known as Kelvin probe force microscopy (KPFM) has emerged as a means of elucidating properties of monolayer films through surface potential mapping.[13] The surface potential of a SAM is strongly influenced by factors such as the packing density, chain conformation, and orientation with respect to the substrate. During KPFM operation, the potential difference between the scanning probe tip and the substrate is measured locally while the probe is held several tens of nanometers from the surface,[14] resulting in a measurement that is not affected by surface texture. Others have shown that this technique is useful for differentiating one SAM molecule from another[15,16] and useful in detecting low-level wear[17] of monolayer films; however, in all cases the studies were carried out on atomically smooth silicon and therefore do not necessarily reflect the influence of surface roughness. The present work aims to show that Kelvin probe force microscopy is well-suited to probe molecular assembly of alkylsiloxane monolayers on rough surfaces and allows one to expand the scope of monolayer growth studies to encompass growth on rough surfaces frequently encountered in real devices.[18]

Previous studies of OTS growth on smooth Si(100) surfaces have shown that growth proceeds in three distinct regimes,[9] separated by well-defined transition temperatures. The existence of these regimes is understood as a consequence of the fact that, in the initial stage of monolayer assembly, the film exists in a near-equilibrium, highly *mobile state* on the water layer wetting the oxidized surface, analogous to the states of the Langmuir film on the surface of water.[2] Eventually, grafting and cross-linking reactions progressively freeze the molecules in their near-equilibrium state, and the final structure of the assembled monolayer is a reflection of its near-equilibrium formation process. In particular, film growth at low temperatures (<16 °C) results in islands of the ordered, densely packed liquid-condensed (LC) phase being frozen on the bare oxide surface. High-temperature growth (>40 °C) proceeds from a completely disordered liquid-expanded (LE) phase with no discernible topographic features with time, and at intermediate temperatures, densely packed islands are intermixed with the expanded phase. Each regime is characterized by changes in molecular arrangement including packing density, chain conformation, and orientation with respect to the substrate; thus it is expected that

† Part of the "Giacinto Scoles Festschrift".

* Corresponding author. E-mail: maboudia@socrates.berkeley.edu.

10.1021/jp075392b CCC: $37.00 © 2007 American Chemical Society
Published on Web 11/10/2007

differences in the conformation of individual alkylsiloxane chains comprising the SAM will alter the monolayer surface potential.

In the present study, we first report on the effect of growth temperature on the surface potential distribution of an OTS monolayer formed on smooth oxidized Si(100) surfaces to provide a basis for studies on rough, polysilicon surfaces, and since similar studies have not been reported to our knowledge. More specifically, *partial* monolayers of the liquid-condensed phase are constructed by quenching monolayer deposition at low temperatures and short reaction times. KPFM measurements enable the direct determination of the local surface potential of the LC phase with respect to the bare substrate. Then, a back-filling procedure, at an elevated temperature, is used to allow for monolayer adsorption in the high-temperature growth regime on the regions not covered during the initial island growth. In this way, the effect of the growth regime on surface potential is studied directly. Our findings support the idea that molecular arrangement becomes increasingly ordered with decreasing deposition temperature and may vary within a single phase as well. The KPFM measurements are then extended to study the growth of assembled monolayers on rough surfaces. While atomic force microscopy cannot differentiate the partial monolayers from the preexisting roughness, KPFM measurements do so readily. It is found that, beyond some roughness, OTS island growth occurs preferentially along grain boundaries in fingerlike monolayers, with local molecular order comparable to that observed on smooth surfaces.

Experimental Section

A. Materials. Octadecyltrichlorosilane (OTS, 90+%), hexadecane, and carbon tetrachloride (both 99+% anhydrous) are purchased from Sigma-Aldrich and used as received. The substrates include Si(100) with a root-mean-square (rms) roughness of ~0.2 nm and polysilicon with rms roughness varied from 2.6 to 10.3 nm. All polysilicon samples are deposited using the Sandia ultraplanar multilevel MEMS Technology (SUMMiT V) process. In this process, n-type, fine-grained polysilicon films are deposited on bare 6 in., n-type Si(100) wafers in a low-pressure chemical vapor deposition (LPCVD) furnace at ~580 °C from silane (SiH_4) gas.[19] The roughness of the polysilicon is varied by means of thermal oxidation in dry O_2 at 900 °C and subsequent etching in hydrofluoric acid. Nanoscale texturing occurs because polysilicon grains are randomly oriented and dry oxidation proceeds at different rates along various crystallographic orientations.[20]

B. Self-Assembled Monolayer Preparation. Sample substrates are cleaned via sonication in acetone, isopropyl alcohol (IPA), and deionized water for 5 min to remove organic contamination. Following sonication, the substrate is ultraviolet ozone (UV-O_3) treated for 5 min, leading to the growth of a chemical oxide with thickness of about 1.5 nm. The sample is then dipped in concentrated hydrofluoric acid for 2 min and subjected to an additional 5 min UV-O_3 treatment to produce a clean, hydroxylated silica surface.

OTS growth is carried out in a controlled environmental chamber with relative humidity held constant at 30% (±2%). Solutions of OTS (~0.5 mM) are prepared in a solvent mixture of 3:2 volume hexadecane/carbon tetrachloride. To grow liquid-condensed islands, the OTS adsorption reaction is allowed to proceed for 5 s at 10 °C, well below the critical temperature for the LC phase in this system.[10] Following adsorption, the samples are quenched in a neat hexadecane/carbon tetrachloride solvent at 10 °C for no less than 1 h. This yields well-formed LC OTS islands on a silica background that is essentially free of OTS molecules.

A back-filling procedure is employed to fill the silica background between islands. With OTS solutions identical to those described above, but reaction temperatures of 25 and 45 °C, the back-filling produces mixed-phase and liquid-expanded monolayers, respectively. Back-filling is allowed to proceed until the water contact angle, measured by the sessile drop method, reaches 110°, indicating complete monolayer coverage. Prior to KPFM imaging, samples are gently wiped with IPA and a cotton swab in order to remove large, bulk polymerized and contaminated debris from the sample surface.

C. Characterization Methods. Atomic force microscopy (AFM) and KPFM are used for characterization of topography and surface potential distribution. The AFM/KPFM instrument (Multimode Nanoscope IIIa with Extender Electronics Module, Digital Instruments) is operated in tapping mode using a Ti−Pt coated silicon cantilever (MikroMasch) with force constant, resonant frequency, and *Q*-factor values of 4.5 N/m, 150 kHz (nominal), and ~200, respectively. A 2.5 V peak-to-peak AC voltage at the resonant frequency of the cantilever is applied between the probe tip and the sample and scanned at frequencies ranging from 0.5 to 1.0 Hz. The resolution of the KFPM system is less than 1 mV.[21] Water contact angles are measured using a Rame−Hart goniometer (model 100-22) in room air using the sessile drop method, with the average measurement error of approximately ±2°.

Results and Discussion

A. Effect of Adsorption Temperature on Surface Potential and Monolayer Ordering. To understand how adsorption temperature effects the surface potential of alkylsiloxane monolayers, it is necessary to examine growth on atomically smooth Si(100). Although temperature-dependent growth of these films has been studied quite extensively by contact angle measurements,[22] by various spectroscopic techniques,[23,24] and by atomic and friction force microscopy,[9,25] here the surface potential is monitored as it varies with microscopic fluctuations in packing and molecular order with respect to the formation of alkylsiloxane SAMs on silicon.

Islands of the liquid-condensed phase are prepared on oxidized Si(100) at 10 °C as described above. Figure 1 shows a representative topographic and surface potential image obtained via AFM and KPFM, respectively. Through water contact angle measurements, it is determined that the adsorption step results in approximately 60% surface coverage (obtained via Cassie's law[26]). As shown in Figure 1, the surface potential of the islands is higher in magnitude than that of the surrounding oxide substrate. Depth distribution profiles are constructed from the topographic and potential data to determine the average height and potential difference associated with the adsorption of the LC phase monolayer. It is found that the average island height is 2.7 ± 0.1 nm (in agreement with the chain length[27]), while the average potential difference is 48 ± 4 mV. From the height data, we conclude that the LC phase monolayer consists of densely packed, straight chains exhibiting low to moderate tilt angles[1] and corresponds to a 48 mV potential shift.

To observe more closely the effects of monolayer adsorption temperature, and, thus, molecular arrangement, on surface potential, a back-filling procedure is employed. This involves the deposition of the expanded or mixed-phase regimes onto regions of the substrate exposed between LC phase islands. It is well-known that high-temperature growth is characterized by random chain conformations and low packing density; thus, one

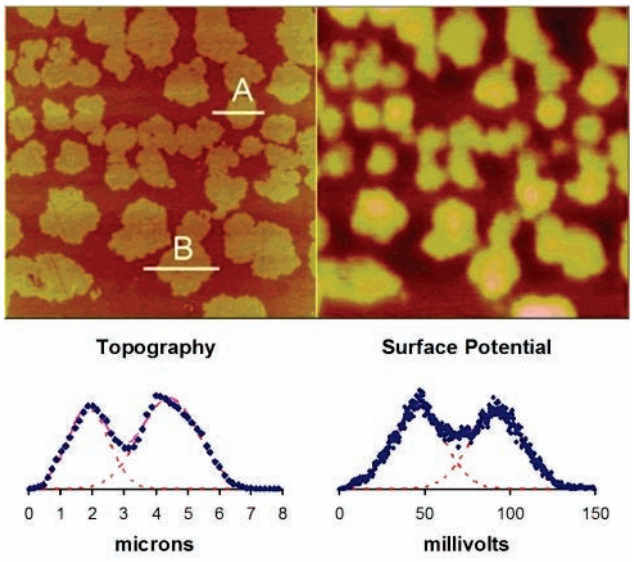

Figure 1. Surface topography (left) and potential (right) for a Si(100) surface partially covered with liquid-condensed OTS islands prepared at 10 °C. Images are 10 × 10 μm with *Z* ranges of 20 nm and 150 mV, respectively. The corresponding feature histograms are also included below each image. Lines A and B denote scan lines used for later analysis (see Figure 3).

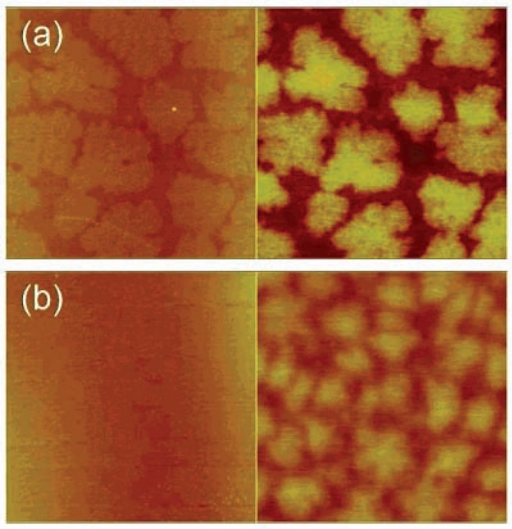

Figure 2. (a) Liquid-expanded phase and (b) mixed-phase back-filled OTS monolayer on Si(100) surface. The left image is topography and the right potential. Images are 10 × 10 μm with relative *Z* scales of 20 nm and 150 mV, respectively.

would expect to observe smaller surface potential values on the basis of the Helmholtz model for the adsorbed layer.[28] This expectation is consistent with the experimental results. Figure 2a depicts the height and potential maps for samples, with LC islands, back-filled at elevated temperatures of ~45 °C. In this scenario, the back-filled region consists exclusively of the liquid-expanded phase and exhibits a chain height and surface potential much lower than that of the liquid-condensed phase. The potential difference between the LE and LC phases is found to be 46 ± 4 mV and, as seen in Figure 2a, a monolayer height less than 2.7 nm, the theoretical chain length.[27]

When the back-filling procedure is carried out at room temperature, a smaller potential difference is measured and sample topography is smooth due to nearly identical OTS monolayer heights. This can be seen in Figure 2b. The surface potential variation between monolayer phases is found to be

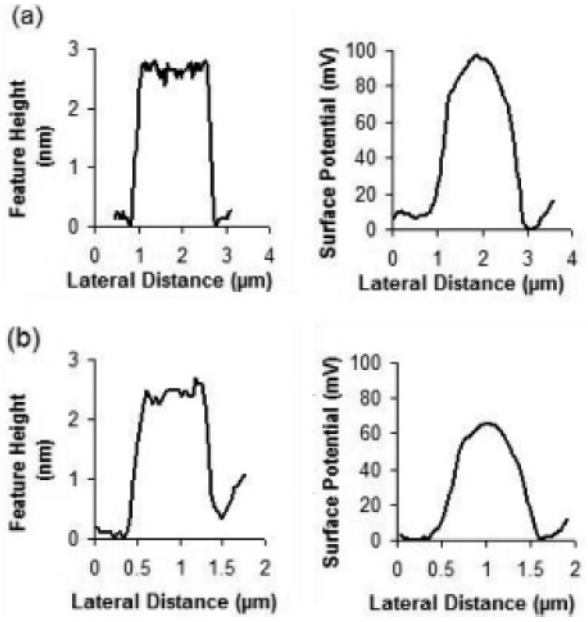

Figure 3. Cross-section profiles for (a) island A height (left) and potential (right) and (b) island B height and surface potential (see Figure 1).

22 ± 4 mV. Thus, a reduced potential at room temperature adsorption suggests that although the OTS monomer chains pack such that they are nearly fully extended, microscopic changes in molecular order are still present. These defects may include a reduced packing density and degree of cross-linking between SAM chains and the substrate, or rotational gauche defects along the SAM backbone, which alter the molecular dipole moment, thereby reducing surface potential. A similar dependence of packing on growth temperature has been previously reported by others for studies conducted using techniques such as contact angle analysis[22] and infrared spectroscopy;[23] however, the methods sample large areas and, hence, are unsuitable for finely probing monolayer adsorption on highly rough surfaces.

Further examination of the potential image in Figure 1 shows that the ordering of the monolayer may vary greatly within a single phase as well. In particular, the surface potential is found to exhibit a maximum at island centers and decrease toward the exterior. This effect appears to be more pronounced for larger islands. LC phase island samples with island sizes ranging from approximately 100 nm to well over 2 μm are investigated by cross-section analysis to elucidate this effect. Figure 3 shows height and surface potential data acquired along the line sections of the two islands "A" and "B" shown in Figure 1. It is readily apparent that although the SAM height is uniform across an island, the surface potential is not and shows a bell-shaped distribution. For the large island with a width of 2 μm (island B) the peak potential value at the island center is greater than 90 mV, whereas for island A of width 1.1 μm the peak potential is only 65 mV. The shape of the potential distribution may indicate that islands are more ordered near the center. This interpretation is consistent with the core−shell hypothesis of Balgar et al., according to which islands are comprised of a cross-linked core surrounded by a weakly bound shell.[10]

By analyzing islands with various sizes, the average island height and average potential shift can be determined as a function of island size. Figure 4 shows that the *average* potential shift associated with the adsorption of LC islands larger than approximately 1.5 μm asymptotes around 50 mV and hence is in good agreement with the potential distribution profiles discussed earlier. However, the average island height achieves

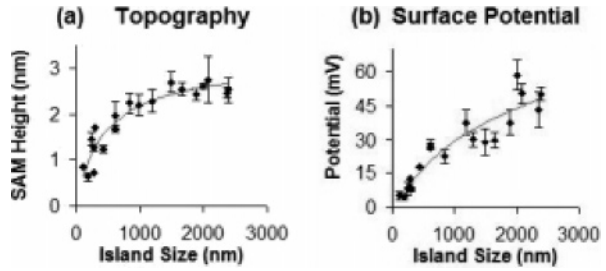

Figure 4. Liquid-condensed island (a) height and (b) potential as a function of island size. The limiting values for island height and surface potential are 2.7 nm and approximately 50 mV, respectively.

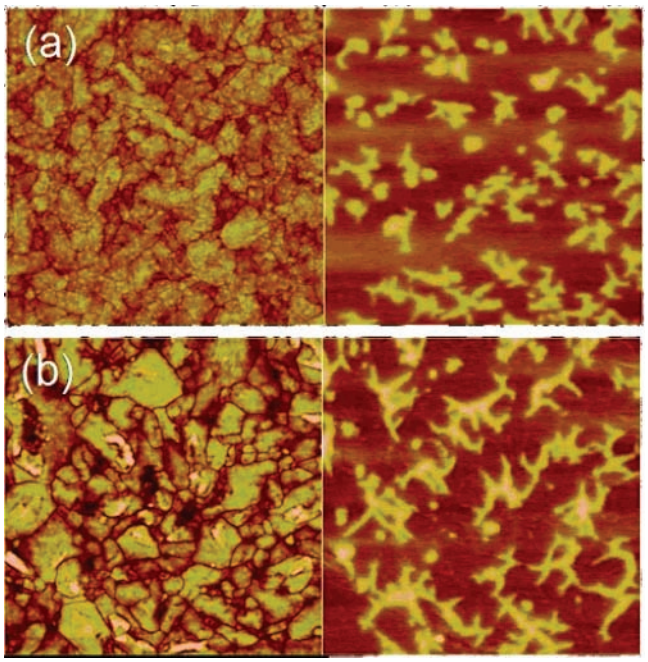

Figure 5. Surface topography (left) and potential (right) for a polycrystalline silicon substrate partially covered with liquid-condensed phase. In a the rms roughness is 2.6 nm and in b 5.6 nm. Note that regions coated by OTS are observable in the potential image, but not in the topography scan, due to the high preexisting surface roughness. Images are 5×5 μm with Z ranges of 25 nm and 150 mV, respectively.

its saturation value of 2.7 nm at a much smaller island size than does the potential. This may be understood when considering that the surface potentials of the liquid-condensed (low-temperature) phase and of the mixed (room-temperature) phase monolayers are quite different despite the heights being nearly identical. This suggests that additional ordering of SAM molecules may occur for islands of intermediate size ($1-2$ μm) even though the full height has been reached. Additional ordering is likely caused by more complete cross-linking or covalent bonding to the substrate, by the elimination of rotational defects along the SAM backbone, or other conformational changes.

B. Growth of Liquid-Condensed Phase on Rough Surfaces. Having characterized the effect of growth temperature and molecular order on the surface potential distributions of OTS monolayers on atomically smooth silicon surfaces, a comparison can be made with those prepared on rough, polycrystalline silicon. The large preexisting surface texture of these surfaces, with roughness values several times that of the monolayer chain length, makes detecting the changes in molecular order of adsorbed alkylsiloxane monolayers through topographic measurements unfeasible. As seen in Figure 5, partial OTS monolayers grown in the LC phase on polysilicon

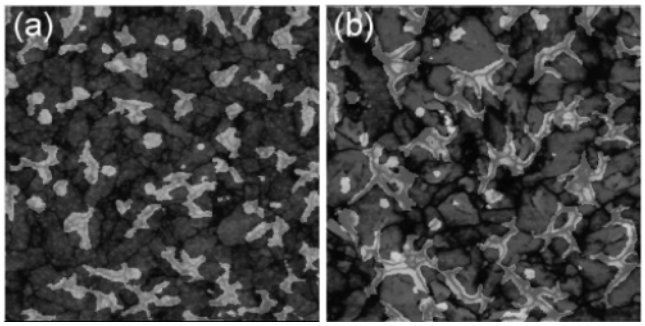

Figure 6. Surface potential image superimposed on the topography images obtained for poly-Si with roughness values of (a) 2.6 and (b) 5.6 nm. Regions of high surface potential are shown in white and consistently overlap grain boundaries. The images are 5×5 μm with Z ranges of 25 nm and 150 mV, respectively.

(rms roughness ranging from 2.6 to 10.3 nm) are not readily observed in an AFM height image. However, one can clearly see the OTS island regions through KPFM surface potential detection. The roughness of the two surfaces is measured via AFM to be 2.6 and 5.6 nm rms, respectively.

Examination of the monolayer morphology shows an interesting phenomenon. As surface roughness increases, island adsorption along grain boundaries becomes more pronounced and they are no longer characterized by circular or dendritic shapes associated with 2D diffusion limited aggregation.[9] Rather, they adsorb in fingerlike monolayers densely packed near surface grain boundaries. This effect is quite pronounced on surfaces exhibiting high roughness (Figure 5b) and becomes less dramatic at moderate to low roughness (Figure 5a). By superimposing the potential and height maps (Figure 6), the effect becomes even more evident. The preferential adsorption of OTS monolayers at grain boundaries is likely due to the presence of a thicker adsorbed layer of water at converging grains. These results are consistent with the nature of Langmuir adsorption.

Finally, depth distribution profiles are constructed as before to elucidate the relative order of OTS partial monolayers adsorbed on these rough surfaces and are compared with the results obtained on smooth Si(100). For islands of the LC phase monolayer, it is found that the average surface potential shift is 52 ± 5.5 mV. This suggests that despite varying growth morphology, the packing density and relative order of the monolayer are comparable to that of the LC phase monolayer on Si(100).

Conclusion

In summary, the feasibility of employing Kelvin probe force microscopy as a means of probing the adsorption and morphology of OTS monolayers grown on both smooth Si(100) and rough polycrystalline silicon has been investigated. It is found that as molecular order and packing density of the SAM molecules increase, the surface potential shift associated with adsorption increases as well. For islands of the liquid-condensed phase of OTS, an average surface potential shift of 48 ± 4 mV is observed. When a back-filling procedure is used to adsorb a disordered, high-temperature growth phase, the potential shift is much lower with the LC phase being 46 and 22 mV greater than the liquid-expanded and mixed-monolayer regimes, respectively. Thus, high surface potentials correspond to a highly ordered phase of OTS monolayer. Furthermore, investigation of OTS islands in the liquid-condensed phase show that surface potential varies across the island cross-section, confirming the core−shell arrangement in which the island core is more ordered than the exterior. Finally, KPFM has enabled imaging of the

OTS monolayer on rough polycrystalline silicon surfaces. In this case, it is found that OTS monolayers grow preferentially along grain boundaries as fingerlike monolayers. These results allow one to expand the scope of adsorbed layer studies onto rough surfaces encountered in many real device applications.

Acknowledgment. The authors acknowledge the financial support of the National Science Foundation, Grant No. DMI-0355339, and of the DARPA Science and Technology Center for Interfacial Engineering for Microelectromechanical Systems (CIEMS).

References and Notes

(1) Ulman, A. *Chem. Rev.* **1996**, *96*, 1533.
(2) Schwartz, D. K. *Annu. Rev. Phys. Chem.* **2001**, *52*, 107.
(3) Mooney, J. F.; Hunt, A. J.; McIntosh, J. R.; Liberko, C. A.; Walba, D. M.; Rogers, C. T. *Proc. Nat. Acad. Sci. U.S.A.* **1996**, *93*, 12287.
(4) Chen, R.; Hyoungsub, K.; McIntyre, P. C.; Porter, D. W.; Bent, S. F. *Appl. Phys. Lett.* **2005**, *86*, 6951.
(5) Färm, E.; Kemell, M.; Ritala, M.' Leskelä, M. *Chem. Vap. Deposition* **2006**, *12*, 415.
(6) Wang, J.; Yan, D.; Xu, Y.; Zhang, J.; Yan, D. *Appl. Phys. Lett.* **2004**, *85*, 5424.
(7) Maboudian, R. *Surf. Sci. Rep.* **1998**, *30*, 209.
(8) Srinivasan, U.; Houston, M. R.; Howe, R. T.; Maboudian, R. *J. Microelectromech. Syst.* **1998**, *7*, 252.
(9) Carraro, C.; Yauw, O.; Sung, M. M.; Maboudian, R. *J. Phys. Chem. B* **1998**, *102*, 4441.
(10) Balgar, T; Bautista, R.; Hartmann, N.; Hasselbrink, E. *Surf. Sci.* **2003**, *532*−*535*, 963
(11) Wang, Y.; Lieberman, M. *Langmuir* **2003**, *19*, 1159.
(12) Fan, F.; Maldarelli, C.; Couzis, A. *Langmuir* **2003**, *19*, 3254.
(13) Lü, J.; Delamarche, E.; Eng, L.; Bennewitz, R.; Meyer, E.; Güntherodt, H. J. *Langmuir* **1999**, *15*, 8184.
(14) Fujihura, M. *Annu. Rev. Mater. Sci.* **1999**, *29*, 353.
(15) Sugimura, H.; Hanji, T.; Hayashi, K.; Takai, O. *Adv. Mater.* **2002**, *14*, 524.
(16) Hayashi, K.; Saito, H.; Sugimura, H.; Takai, O.; Nakagiri, N. *Ultramicroscopy* **2002**, *91*, 151.
(17) DeVecchio, D.; Bhushan, B. *Rev. Sci. Instrum.* **1998**, *69*, 3618.
(18) Maboudian, R.; Carraro, C. *Annu. Rev. Phys. Chem.* **2004**, *55*, 35.
(19) Sniegowski, J. J.; deBoer, M. P. *Annu. Rev. Mater. Sci.* **2000**, *30*, 299.
(20) Zhang, X. G. *Electrochemistry of Silicon and Its Oxide*; Kluwer Academic: New York, 2001; p 114.
(21) Nonnemacher, M.; O'Boyle, M. P.; Wickramasinghe, H. K. *Appl. Phys. Lett.* **1991**, *58*, 2921.
(22) Brzoska, J. B.; Azouz, I. B.; Rondelez, F. *Langmuir* **1994**, *10*, 4367.
(23) Parikh, A. N.; Allara, D. L.; Azouz, I. B.; Rondelez, F. *J. Phys. Chem.* **1994**, *98*, 7577.
(24) Chow, B. C.; Ehler, T. T.; Furtak, T. E. *Appl. Phys. B* **2002**, *74*, 395.
(25) Tian, F.; Xiao, X.; Loy, M. T. T. *Langmuir* **1999**, *15*, 244.
(26) Cassie, A. B. D.; Baxter, S. *Trans. Faraday Soc.* **1944**, *40*, 546.
(27) Stevens, M. J. *Langmuir* **1999**, *15*, 2773.
(28) Taylor, M.; D.; Bayes, G. F. *Phys. Rev. E* **1994**, *49*, 1439.